Experimental Investigations on Focusing of Weak Spherical Shock Waves in Water by Shallow Ellipsoidal Reflectors

by M. Müller
Stoßwellenlabor, Institut für Luft- und Raumfahrt
der Rheinisch-Westfälischen Technischen Hochschule Aachen

Summary

Spherical shock waves, generated by an underwater spark discharge in the first focus of an ellipsoid, are focused after reflection from an elliptical surface in the second focus.

Shadowgraphs give an impression of the propagation and converging process, whereas for the pressure measurements special pressure probes with a high temporal and spatial resolution had to be designed to allow investigations up to the focal "spot". Hence it can be shown, that reflector parameters like diameter, focal length and material cause a great influence on the focusing process and the pressure amplification. Using a brass reflector with a diameter to focal length ratio of $D/f = 3$, the focal pressure rises up to 1300 bar, corresponding to an amplification of about 100 compared to the incident wave at the reflector surface.

After reflection from a soft reflector, one can get converging expansion waves, which generate tensions up to -80 bar.

Experimentelle Untersuchungen zur Fokussierung schwacher sphärischer Stoßwellen in Wasser durch flache, ellipsoide Reflektoren

Zusammenfassung

Sphärische Stoßwellen, erzeugt durch eine Unterwasserfunkenstrecke im ersten Fokus flacher Ellipsoidsegmente, werden nach der Reflexion an der ellipsoiden Oberfläche im zweiten Brennpunkt fokussiert. Schattenaufnahmen ermöglichen die qualitative Beurteilung des Konvergenzprozesses, während zur quantitativen Beschreibung eigens Drucksonden mit hoher zeitlicher und räumlicher Auflösung entwickelt werden mußten, die Messungen bis in den Fokusbereich erlauben. Dadurch kann gezeigt werden, daß die Reflektorparameter wie Durchmesser, Brennweite und Material einen wesentlichen Einfluß auf die Amplitude im Fokus besitzen. Durch Verwendung eines Messingreflektors mit einem großen Durchmesser-zu-Brennweite-Verhältnis sind Fokusdrücke bis zu 1300 bar erzielbar, entsprechend einer Verstärkung von 100 gegenüber dem einfallenden Stoß. Durch Reflexion an schallweichen Reflektoren erhält man konvergierende Expansionswellen, die Spannungen bis zu -80 bar erzeugen.

Recherches expérimentales sur la focalisation dans l'eau d'ondes de choc sphériques, d'amplitudes modérées, par des réflecteurs ellipsoïdaux peu profonds

Sommaire

Des ondes de choc sphériques sont produites dans l'eau par une décharge électrique localisée au premier foyer d'une surface ellipsoïdale et focalisées au second foyer de la même surface après réflexion sur un miroir épousant la forme d'une partie peu profonde de ladite surface ellipsoïdale.

Des ombrogrammes donnent un aperçu des processus de propagation et de convergence des ondes de choc avant leur arrivée au second foyer, tandis que des sondes de pression à hauts pouvoirs de résolution temporelle et spatiale, spécialement mises au point pour ces expériences, permettent des mesures de pression jusqu'à l'intérieur même de la tache de focalisation. On a pu montrer de cette manière que certains paramètres caractéristiques des réflecteurs, comme par exemple le diamètre, la distance focale ou le matériau constitutif, exerçaient une grande influence sur le processus de focalisation et l'amplification de pression qui en résulte. Un réflecteur de laiton d'un rapport diamètre/distance focale égal à 3 a fourni des surpressions focales de 1300 bar, correspondant à une amplification par un facteur 100 de la pression de l'onde incidente au niveau de la surface même du réflecteur.

Une réflexion par un miroir en matériau acoustiquement mou peut conduire à des ondes d'expansion générant des tensions (pressions négatives) jusqu'à -80 bar.

1. Introduction

If a shock front is curved or it reflects at a concave surface, the front normals will cross and an amplification of energy density arises. First investigations on the field of shock wave focusing were carried out in air by Sturtevant and Kulkarny [1] with shock tube experiments. R. Holl [2] made experiments using ellipsoidal reflectors and short blast waves in air with amplitudes up to $\Delta p = 0.3$ bar.

corresponding to a Mach number of $M = 1.13$. Both authors got a decreasing amplification in the focal region with increasing Mach number, which was explained by the nonlinear behavior of the shock wave propagation during the focusing process. Only for very weak shock waves like acoustic waves high amplifications up to 40 or 50 of the incident wave were observed [2].

Using a comparable amount of energy in water, pressure pulses with amplitudes of several hundred bars are reached, since the density does not change very much. The wave propagation velocity also does increase very little with increasing pressure. Hence in the gas dynamic sense shock waves in water up to a few hundred bar can be regarded as rather weak, and, during the focusing process, very high pressure intensifications should occur. Compared with the acoustical theory, where infinite amplitudes in the focus arise, the real amplifications will be limited by small nonlinearities.

Since the high pressure amplitudes open a far field of useful applications, for example on the field of medical treatment, a worldwide interest on shock wave focusing has arisen in recent years, both on experimental research [3–7] and on computational work [8–11]. In both cases, the limits of modern measurement techniques and computational limits were reached. The reason for that is found in the high propagation velocity of about 1500 m/s as well as in the short pulse length of only a few microseconds [12]. These facts request measurement systems with an extremely large temporal and spatial resolution. These difficulties could be reduced by the development of a miniature pressure probe on the base of the piezoelectric polymer pvdf (polyvinylidene fluoride) [13]. With its short rise time in the order of 50 ns and its spatial resolution less than 500 μm measurements are possible up to the focal "spot".

On this basis a systematic investigation of shock wave focusing has been carried out. In the first period the basic phenomena of shock wave focusing will be made evident and the influence of reflector parameters like diameter, focal length and reflector material on the focusing process will be studied. For this purpose, a number of shallow ellipsoidal reflectors are used. Compared to deep reflectors, which are used in the field of medical treatment, deviations of regular shock wave reflection from the acoustic behavior are negligible as well as unknown wall effects, because the incident angles of the front normals are very low [11] and any disturbance of the converging front by the initial shock is avoided. So the main interest can be concentrated on the focusing process itself, which will be visualized by a shadowgraph system. The pressure history will be measured at different positions in the converging field.

2. Calculating shock waves in water

Shock waves in water are mainly described by using the modified Tait-equation suggested by Kirkwood et al. [14]

$$\varrho(P, T) = \varrho(0, T)\,(1 + p/B)^{1/n}. \tag{1}$$

As Holl [2] has shown the density ratio can be obtained according to

$$\frac{\varrho_2}{\varrho_1} = \left(\frac{P_2 + B}{P_1 + B}\right)^{1/n} \tag{2}$$

namely $(P + B)/\varrho^n = \text{const.}$, where he made use of the relation

$$\frac{\varrho(0, T_2)}{\varrho(0, T_1)} \approx 1 \quad \text{for} \quad 293\,^\circ\text{K} < T < 333\,^\circ\text{K}. \tag{3}$$

B is a function of temperature but does not vary very much. For room temperature of 20 °C B yields to 2955 bar; n is also nearly constant in the considered range of pressure and temperature and is chosen in such a way, that the correct sound speed $a = 1483$ m/s for room temperature can be calculated. The sound speed for water is given by

$$a = \left(n\frac{p + B}{\varrho}\right)^{1/2} \tag{4}$$

which leads to $n = 7.44$.

Introducing the modified pressure $p' = p + B$ and n instead of the isentropic coefficient γ for gases, it was shown that all the gasdynamic equations can be transformed to hydrodynamic equations, since the shock wave pressure keeps less than $p_2 = 10$ kbar [2].

Using this transformation the Mach number for a shock wave of an amplitude of $p_2 = 20$ bar is calculated with

$$M = \left(\frac{(n + 1)\,p'_{21} + n - 1}{2n}\right)^{1/2} \tag{5}$$

and

$$p'_{21} = p'_2/p'_1 = (p_2 + B)/(p_1 + B) \quad \text{to} \quad M = 1.0018.$$

This shows, that shock waves in water with a quite high pressure amplitude compared to gaseous mediums, are rather weak in the gas dynamic sense, and the reflection and focusing of such a water shock should obey rules very close to the theory of the geometrical acoustic.

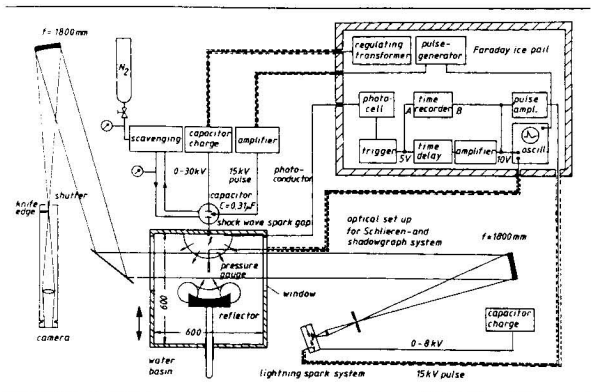

Fig. 1. Experimental arrangement.

3. Experiments

3.1. Experimental arrangement

The experiments in focusing spherical shock waves are carried out in a water basin with $(600 \times 600 \times 800)$ mm^3 (Fig. 1). The basin wall is doubled to avoid vibration and to get a maximum of attenuation of the shock wave at the basin wall. Between the inner boundary, made of a plastic material with a low acoustical impedance to water and the outer one of aluminium, 40 mm of a fine sand is filled to absorb the transmitted shock waves. Inside the wall two aluminium blocks are fitted for mounting the shock generator and the ellipsoidal reflectors. Perpendicular to these, two large windows with $(345 \times 205 \times 19)$ mm^3 are mounted, which allow to visualize the complete propagation process.

The basin is filled through the bottom, so that bubble free water, which has been deionized and degassed before, is guaranteed.

The generation of the shock wave is obtained by an underwater spark gap, fixed in one of the aluminium blocks. One electrode, made of spring steel, is formed like a hook. The other is of tungsten/copper 80/20 and inserted in the metal wall. A defined discharge is guaranteed using a tip to tip arrangement. A schematic drawing of the spark gap and the obtained shock front is given in Fig. 2.

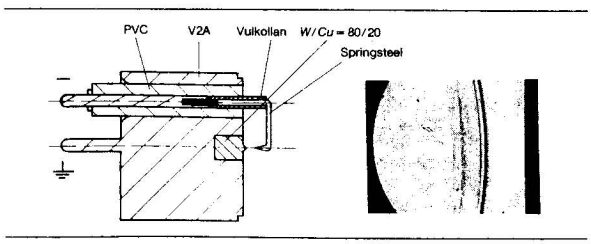

Fig. 2. Spark gap and a shadowgraph of the generated shock front.

To obtain a fast energy transfer a low total inductivity of the electrical circuit is necessary. Using a compact coaxial form and a direct mounting to the capacitor an inductivity of only $L = 106$ nH is attained. To approach a point source of the blast wave the distance of electrodes is chosen to $d = 2$ mm. The voltage of the capacitor ($C = 0.31$ µF) is $U_0 = 20$ kV. The efficiency of energy transfer from electrical to the shock wave energy is about 2.5%.

3.1.1. Measurement techniques

The visualization of the propagation and the focusing process is carried out by a single shot schlieren system (s. Fig. 1). The flash light is triggered through an adjustable delay after the shock wave generation, so that different shock wave positions can be photographed. The exposure time is about 1 µs. To obtain a correct delay time the moment of the main spark discharge is measured by a photocell. This is necessary because there is always a various delay time between the trigger signal from the pulse generator and the moment of discharge, which increases with increasing distance of electrodes and decreasing voltage.

The parallel light beam in the test section has a diameter of 178 mm (s. Fig. 1). It is focused by a second spherical mirror with a focal length of $f = 1800$ mm, passes a knife edge in the focus position, which screens the deviations from parallel light by the shock wave, so that we shall get black lines on the polaroid film (ASA 3000) in the camera.

Since the focusing process is three-dimensional and optical systems like holographic interferometry do not give the necessary resolution in the focal area [5], the pressure histories can only be recorded by specially designed pressure gauges. As Eisenmenger [12] has shown, shock waves in water only have rise times of the order of nanoseconds, so that for a quantitative measurement of the focusing process the pressure probes have to fulfill special requirements:

- large pressure range (up to 2000 bar),
- high spatial resolution (→ focus region),
- minimum of rise time (~ 10 ns).

As commercial pressure probes with these specifications are not available a pressure probe which combines all these requirements was designed. In cooperation with M. Platte [13] a micro pressure gauge was constructed on the base of an ordinary needle and the piezoelectric polymer polyvinylidene fluoride (pvdf) (Fig. 3).

The needle is coated with a thin layer of liquefied pvdf which, after solidification, is polarized at

Table I.
Data of the reflectors used.

Reflector	Material	R %	a mm	b mm	e mm	l mm	t mm	α	f mm	D mm	D/f
I	brass	0.92	60.0	56.6	20.0	80.0	17.6	65.3°	40.0	80.0	2.0
II	brass	0.92	211.9	152.7	146.9	358.8	48.8	34.9°	65.0	195.0	3.0
III	steel	0.94	244.4	216.0	114.4	358.8	26.3	32.7°	130.0	195.0	1.5
IV	steel	0.94	244.4	216.0	114.4	358.8	49.2	45.5°	130.0	260.0	2.0
V	foam of pu	−0.97	244.4	216.0	114.4	358.8	26.3	32.7°	130.0	195.0	1.5
VI	foam of pu	−0.97	211.9	152.7	146.9	358.8	48.8	34.9°	65.0	195.0	3.0

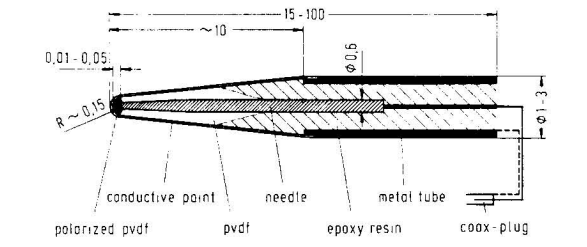

Fig. 3. Cross section of the "needle probe".

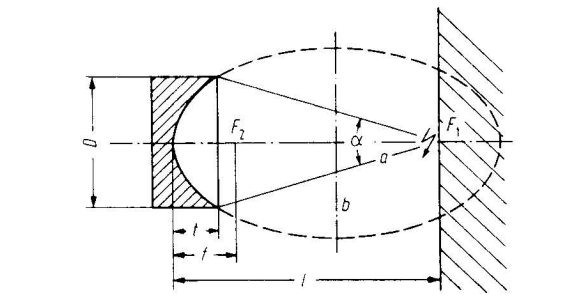

Fig. 4. Schematic cross section of the experimental set up.

the top by a corona discharge. Its thickness at the top is between 10 and 50 µm, the diameter less than 500 µm. One contact is the needle itself, the other is a thin layer of silver conductive paint and a metal tube.

In a plane wave field, a constant sensitivity of 3 dB up to 10 MHz was found. The rise time is in the order of $10 \cdots 50$ ns. By calibrating the probes in a water shock tube a linear sensitivity up to 320 bar could be verified. The values vary between 0.05 pC/bar up to 0.4 pC/bar.

3.2. *Reflectors*

For focusing spherical shock waves six different ellipsoidal reflectors are used. They are located on the opposite side to the spark gap in a position, that the centre of the shock wave coincides with one focus of the reflector.

Fig. 4 and Table I show the schematic cross section of the experimental arrangement and the data of the tested reflectors, respectively. That part of the hemispherical shock wave, inside the angle α, which encounters the reflector surface, will propagate towards the second focus F_2 after reflection.

Four of the reflectors are made of a material with a high acoustical impedance compared to water with a coefficient of reflection of $R = 92 \cdots 94\%$ of the incident pressure, to study the focusing of compression waves, whereas two reflectors are made of polyurethane foam, which has a very low acoustical impedance to water. At its smooth surface incident shock waves will be reflected as expansion waves, which are focused during the converging process. All reflectors with the exception of reflector I, for which a pressure measurement is not possible because of its small distance to the spark discharge have a distance to the origin of the blast wave of about $l = 360$ mm; they differ in diameter, focal length and material.

3.3. *Experimental results*

The converging shock fronts and the focal regions of all reflectors except I, are measured on the whole length of the axis of symmetry and perpendicular to that along the shock fronts. The positions of the shock wave front are photographed at various times for each reflector and give an informative qualitative impression of the focusing process. Besides that, the shadowgraphs give the possibility of a correct locating of the pressure probe normal to the shock front.

Fig. 5 shows the propagating wave fronts after reflection for the reflector II, III and V, respectively. The incident shock waves have propagated from the right to the left; the black area on the left is the silhouette of the reflector edge. The dark concave part represents the reflected front on its way to the focus, the fine convex lines in the upper and lower part of the picture show the diffracted wave generated at the reflector edge. The focus is reached in the

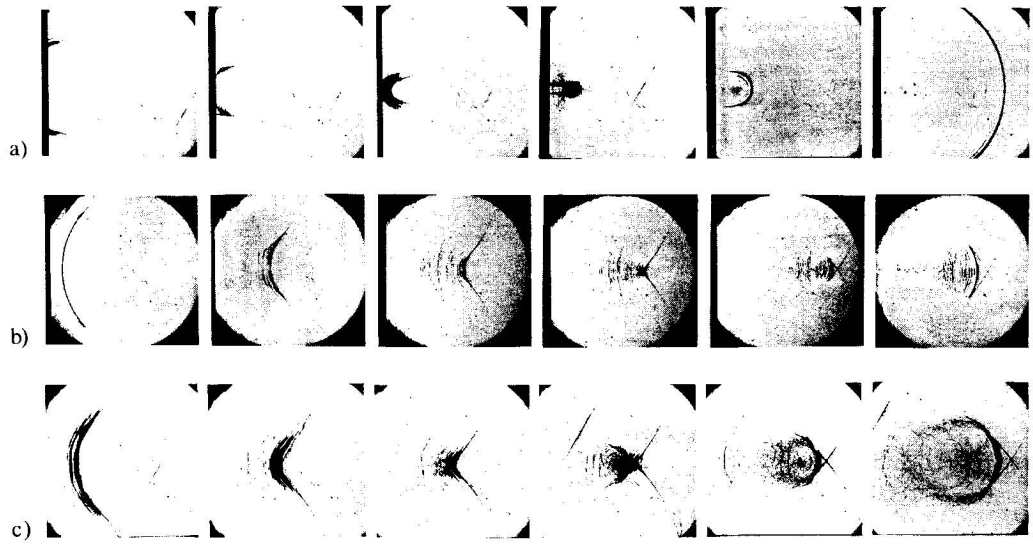

Fig. 5. Shadowgraphs of the focusing process; illuminated diameter 178 mm.
a) reflector II; b) reflector III, and c) foam reflector V.

fourth picture. Afterwards the front diverges again in the same way as it converged before. Later the crossing of the diffracted wave in front of the main shock is visible and some small cavitation bubbles appear in the focus region. As the waves are rather weak the reflection takes place according to the geometrical acoustics and the focus coincides with the geometrical one. This is representative for all tested reflectors with a high acoustical impedance, whereas in addition the foam reflector (Fig. 5 c) shows some special effects in the focal region. As the tension in that area grows, a lot of small bubbles appears, which collapse again a few microseconds later and generate small spherical shock waves. In the focal region a complete chain of these cavitation bubbles are generated. They collapse again nearly at the same time and cause a new pressure distribution which, as an envelope of all the single fronts, can be seen on the shadowgraph as a dark ring. Since the precursing expansion wave propagates a little slower than the generated pressure wave, it will be passed as it is clearly seen in the fifth shadowgraph.

As an example for the pressure distribution in the focusing field Fig. 6 shows the pressure history of reflector III. The positions of the shock front together with the diffracted wave generated at the reflector edge (——) are plotted for three different times. The diffracted expansion wave from the reflector edge is drawn as a dashed line (– – –).

The left oscillogram in the middle shows the pressure profile of the incident shock wave without a reflector. This blast wave has an amplitude of about $\hat{p}_0 = 11$ bar. 2/3 of the amplitude are reached after a rise time of about 50 ns; the complete rise time to the maximal peak is about 250 ns. The following exponential decay has a time constant of 3 µs.

The upper profiles describe the pressure history on the axis of the reflector. The considerable amplification up to the focal "spot" is clearly demonstrated. The pulse length is shortened to only 400 ns by a rise time of only a few nanoseconds. The amplitude is 54 times as high as the incident wave at the location of the reflector surface, that means about 600 bar. The expansion wave generated at the reflector edge is recorded as a negative peak, which pursues the precursing shock front and leads to a negative pressure of about − 30 bar near and at the focus.

The lower oscillograms show the pressure distribution at a distance to the reflector axis. The middle profile gives the amplitude at the focus and on a line normal to the axis; at a distance of 1 mm to the focus there are 60% left, 2 mm beside only 35% of the amplitude at the focus. Along the front the pressure amplitude has its maximum value about 2/3 of the distance from the axis to the marginal beam. In the acoustic ray theory the maximum should be on the marginal beam as a matter of geometry. But in reality the shock in this area is weakened by diffraction and the following expansion wave.

The details of the pressure distribution in the diverging part behind the focus together with the crossing over of the diffracted waves are given in Fig. 7. The "needle probe" can be located parallel to the reflector axis, because its sensitivity as a function of angle of incidence is very low [13]. The

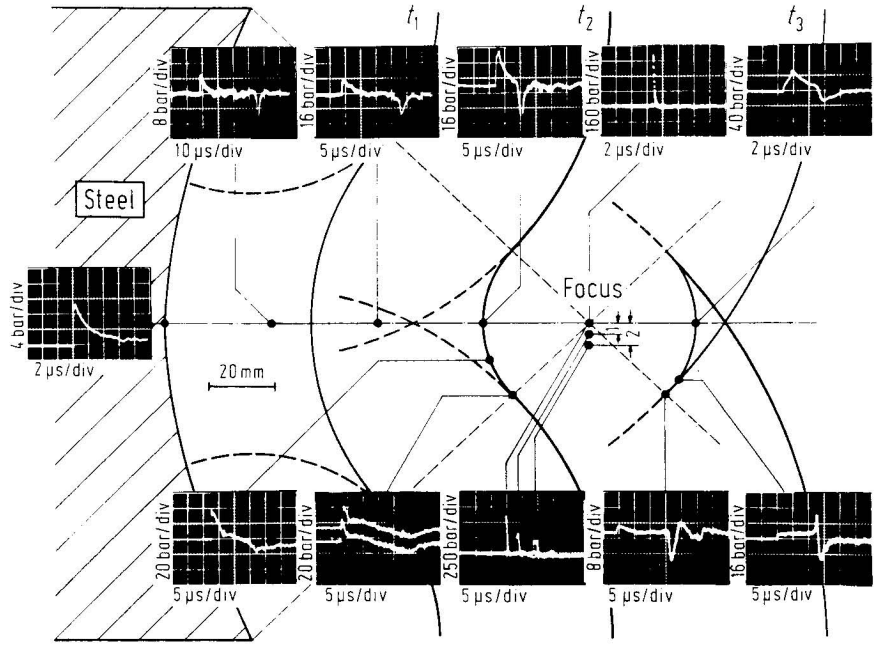

Fig. 6. Pressure distribution in the focusing field of reflector III. Energy of capacitor $E_c = 62$ J.

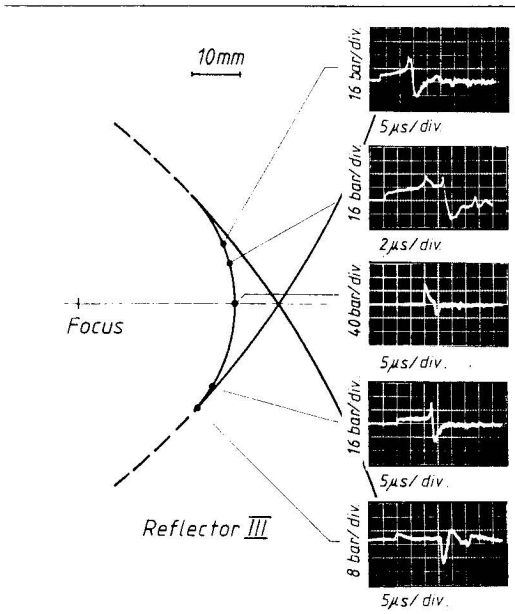

Fig. 7. Pressure distribution of the diverging front behind the focus; reflector III.

pressure probe is hit by three fronts which can be clearly resolved. The upper profiles show, that the first front shifts the pressure to a value of about 8 bar, which rises very slowly until the second front reaches the probe. There is only a small decay between the second and the main front, which has nearly the same amplitude as the second one. This means, that the pressure region is bounded by the small triangle. The main front is directly followed by a sharp expansion which is clearly recorded on all oscillograms. The negative peak has its maximum on the axis.

Reflector V with the same geometry as III, but made of the soft material generates very similar but inverse pressure profiles. The negative response is very sharp with a rise time less than 1 µs. Though, the following diffraction wave, in this case a pressure wave, cannot be seen very well. As an example Fig. 8 shows the pressure distribution at and near the focus together with the position of the pressure gauge. The upper profile gives the tension at the focus. One can see a short rise time of about 200 ns to an amplitude of about -90 bar, which is followed by a short pressure phase. Figs. 8 b, c were made in positions 2 and 5 mm beside the focus. The amplitude falls down very rapidly, which means, that this focal area is also very small. It is followed by a sharp positive peak, which can be seen on the schlieren photograph as a white line. The lower pictures are made 21 mm behind the focus and 21 mm beside. Even here the profile is very similar to the oscillogram presented in Fig. 7, only upside down.

The highest amplification is reached by reflector II with a comparatively large diameter to focal length ratio of $D/f = 3$ (Figs. 9 a, b). Its focus pressure rises up to 1300 bar, which is more than

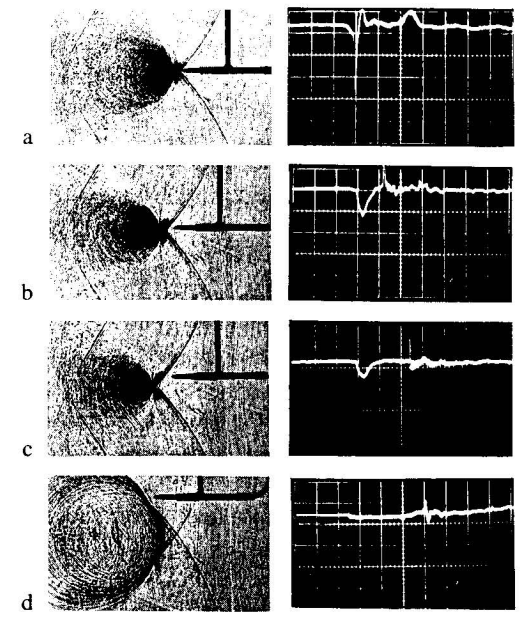

Fig. 8. Shadowgraphs and location of the pressure probe together with the obtained pressure distribution in each position; foam reflector V; vert.: 30 bar/div. horiz.: a–c) 2 µs/div, d) 5 µs/div.

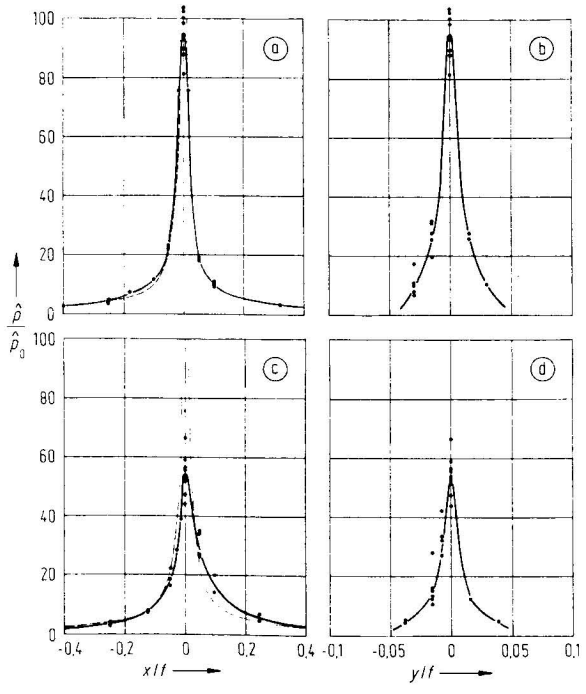

Fig. 9. Pressure distribution on axis of symmetry (x) and on a line normal to the axis (y) at the focus ($x/f = 0$) versus distance from focus; reflector surface $x/f = -1$; $\hat{p}_0 = 11$ bar; (—●—) experiment, (– – –) geom. acoustic.; (a, b) reflector II; (c, d) reflector III.

100 times the pressure on the reflector surface. As predicted the pressure distribution differs only in the focal region from the acoustic theory (dashed line) and no deviation between the locus of the maximum on-axis pressure and the geometrical focus is observed. This is valid for all tested reflectors with a high acoustical impedance. The dimension of the focal region is very small and the pressure drops very sharply perpendicular to the reflector axis. The pressure approaches to zero at 5% of the focal length (Fig. 9 b).

The same dimensionless pressure distribution perpendicular to the axis is obtained for the other reflector geometries, for example by using reflector III (Fig. 9 d). But this means, that the same shock wave energy is concentrated on a larger focal region, here nearly the double range. So the maximum peak pressure will decrease; in this case to only 54% the incident wave (Fig. 9 c). If we compare the different amplifications reached by different reflector geometries, we will see, that the pressure maximum increases with increasing D/f or decreasing f (Fig. 10). The reason for this effect are small nonlinearities during the focusing process, which have more influence on longer ways to the focus. So the focal region grows and the energy density decreases.

The comparison between reflector III and IV which have the same focal length but different diameters shows a correlation between reflector size and focus pressure. Since the lateral dimension at the focus is the same for both reflectors (up to 5% of f), the focus pressure should rise proportional to the surface extension. The energy density per unit area is proportional to p^2 and the reflector surface of reflector IV is $A_{IV} = 1.77 \times A_{III}$. Hence the focus amplification should grow in this approximation from 54 for reflector III to 72 for reflector IV. An average of about 75 is measured which verifies the

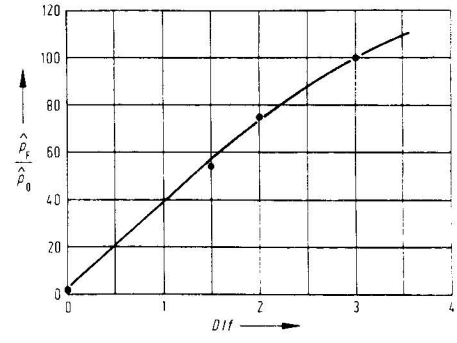

Fig. 10. Pressure amplification at the focus as a function of convergency D/f; $l = 358{,}8$ mm; $\hat{p}_0 = 11$ bar.

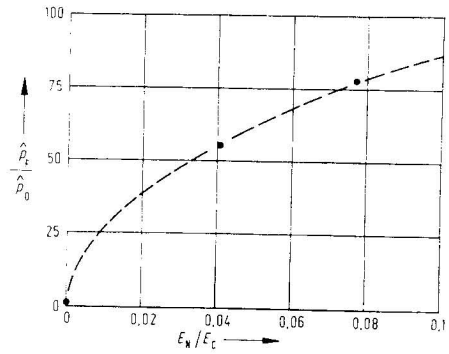

Fig. 11. Pressure amplification at the focus as a function of utilized shock wave energy E_N; E_c = const. = 62 J; $\hat{p}_0$ = 11 bar.

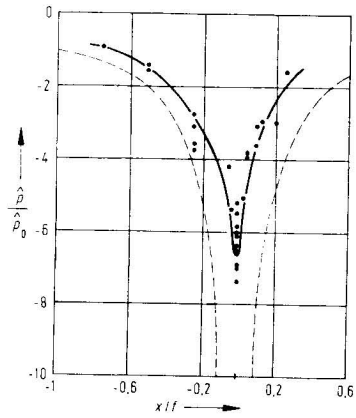

Fig. 12. Pressure distribution on the axis of symmetry versus distance from focus; reflector V; $\hat{p}_0$ = 11 bar; (—●—) experiment, (– – –) geom. acoustic.

prediction very well. Fig. 11 shows the measured amplifications for the two different reflectors as a function of the efficient shock energy to the complete energy of the hemispherical blast wave.

Fig. 12 gives the pressure amplitude on the reflector axis for the soft reflector V. Even here the maximum amplitude is measured at the geometrical focus and values between −70 to −90 bar are obtained, according to an amplification of about 7. It is limited to this low value because cavitation arises and the homogeneous state of the water is disturbed. The difference between experiment and theory illustrates the dissipation effect, caused by the development of small vapour bubbles.

4. Discussion

The experimental results show, that the focusing process of very weak shock waves in water of only several bar pressure amplitude is quite well predictable by the theory of the geometrical acoustics with the exception of the focal region. For these waves no nonlinear behavior is visible. On the other hand the pressure amplitude at the focus is limited by small nonlinearities. Its peak grows with an increasing diameter to focal length ratio D/f. That means, that a very sharp focus with a very high pressure can be reached by using a large reflector with a short focal length.

In comparison with similar experiments in air made by Holl very good agreement both qualitative and quantitative is found. His measured pressure amplifications between 40 and 50, using a Mach number of $M = 1.004$ and a similar reflector to reflector III, are also reached, as well as an agreement in the pressure distribution along the axis and perpendicular to it. Hence the theoretical transformability from air to water shocks proposed by Kirkwood [14] and Holl [2] is verified. In air the first nonlinear effects appear for an incident shock Mach number of about $M = 1.03$ [1, 2]. This is equivalent to a pressure amplitude in water of about 320 bar (eq. 5). Nevertheless the measurement of the real amplitudes, in order to claim its application field, has to be done with the original reflector.

In water the only comparison that can be made is with experiments made by Takayama et al. [5]. They used a similar configuration and a shallow reflector with $D/f = 2.67$ and $D = 50$ mm. The incident shock was measured to less than 20 bar. The measurement was made by holographic interferometry and showed a qualitative agreement with our experiments. Since the front due to the weak incident pressure should propagate similar to the geometrical acoustic, the maximum pressure should occur near the geometrical focus. However, the maximum pressure of about 800 bar was achieved about $0.3f$ in front of the focus, so this discrepancy in the result of their work remains to be verified.

The comparison to computational simulations of the shock wave focusing in water using the Random-Choice-Method by Olivier [8, 9] and the piecewise-linear method by Sommerfeld [11] shows good agreement with the exception of the pressure amplification in the focus region. They also reach the on-axis maximum at the locus of the geometrical focus but the sharpness of the focus cannot be simulated as a matter of the relatively large grid size due to finite computer capacity, which leads to a wider focus and a lower amplitude.

Using soft reflectors it could be shown, that stress in water is transferable up to amplitudes of about −80 bar. This probably opens a new range of applications in cases where focused pressure waves

are not effective. In order to reach manipulations on materials with a similar acoustical impedance to water like human body tissue, for example cancer cells, this technique could be helpful in medical treatment.

Especially together with the hundreds of small cavitation bubbles produced on the trace of the focusing expansion wave, which generate high intensive micro shock waves and micro liquid jets in the direction of boundaries, these stress waves might affect soft materials.

Focused shock waves are already used in medical applications for fracturing kidney stones. For this purpose half ellipsoidal reflectors are used, which utilize about 90% of the generated shock wave, whereas in our cases only 4 to 7% of the hemispherical blast wave were focused. In order to make investigations using deep ellipsoidal reflectors a second series of experiments is prepared. Since the converging angle of the focusing shock is lower compared to the considered cases above, a bigger influence of small nonlinearities will appear. Together with unknown wall effects and since the reflected front propagates into a disturb flow field by the precursing shock, no such sharp focal regions will be expected. On the other hand the reflector surface is much larger, so that higher pressure amplitudes could be finally achieved.

Acknowledgements

I would like to thank Prof. Dr. rer. nat. H. Grönig for his encouragement, his helpful discussions during this work and not least for reading the manuscript.

This research is partially supported by the Deutsche Forschungsgemeinschaft through Sonderforschungsbereich 27 "Wellenfokussierung".

(Received 17th October 1986.)

References

[1] Sturtevant, B. and Kulkarny, V. A., The focusing of weak shock waves. J. Fl. Mech. **73** [1976], 651.
[2] Holl, R., Wellenfokussierung in Fluiden. Dissertation, Aachen, 1982.
[3] Chaussy, Ch., Forßmann, B., Brendel, W., Jocham, D., Eisenberger, F., Hepp, W., and Gokel, J. M., Berührungsfreie Nierensteinzertrümmerung durch extrakorporal erzeugte, fokussierte Stoßwellen. Reihe: Beitr. zur Urologie Bd. 2. Karger-Verlag, München 1980.
[4] Müller, H. M. and Grönig, H., Fokussierung von Stoßwellen in Wasser. Forschungsberichte SFB 27, 1982 u. 1985 (Internal reports).
[5] Takayama, K., Esashi, H., and Sanada, N., Propagating of spherical shock waves produced by underwater microexplosions. R. D. Archer and B. E. Milton (eds.): 14th Int. Symp. on Shock Tubes and Waves, Sydney 1983, p. 553.
[6] Russel D. A., Shock dynamics of noninvasive fracturing of kidney stones. D. Bershader (ed.): 15th Int. Symp. on Shock Waves and Tubes, Berkeley 1985.
[7] Müller, H. M. and Grönig, H., Experimental investigations on shock wave focusing in water. Proc. 12th Int. Congr. on Acoustics Vol. III, H3-3 Toronto 1986.
[8] Olivier, H., Zweidimensionale instationäre Stoßwellen. Anwendung der Random-Choice Methode. Dissertation, Aachen 1985.
[9] Olivier, H. and Grönig, H., Two-dimensional shock focusing and diffraction in air and water. D. Bershader (ed.): 15th Int. Symp. on Shock Waves and Tubes, Berkeley 1985.
[10] Nishida, M., Nakagawa, T., Saito, T., and Sommerfeld M., Interaction of weak shock waves reflected on concave walls. D. Bershader (ed.): 15th Int. Symp. on Shock Waves and Tubes, Berkeley 1985.
[11] Sommerfeld, M. and Müller, H. M., Experimental and numerical studies of shock wave focusing in water. Submitted to Experiments in Fluids.
[12] Eisenmenger, W., Experimentelle Bestimmung der Stoßfrontdicke aus dem akustischen Frequenzspektrum elektromagnetisch erzeugter Stoßwellen in Flüssigkeiten bei einem Stoßdruckbereich von 10–100 atm. Acustica **14** [1964], 187.
[13] Müller, H. M. and Platte, M., Einsatz einer breitbandigen Piezodrucksonde auf PVDF Basis zur Untersuchung konvergierender Stoßwellen in Wasser. Acustica **58** [1985], 215.
[14] Kirkwood, J. G., Bethe, H., Montroll, E., and Richardson, J. M., The pressure wave produced by an underwater explosion. OSRD Reports I (No. 588), II (No. 676) and III (No. 813).